Hindawi Publishing Corporation
Journal of Quality and Reliability Engineering
Volume 2016, Article ID 9184039, 7 pages
http://dx.doi.org/10.1155/2016/9184039

Research Article

Physicochemical Characterization of Alginate Beads Containing Sugars and Biopolymers

Tatiana Aguirre Calvo[1] and Patricio Santagapita[1,2]

[1]*Industry Department and Organic Chemistry Department, Faculty of Exact and Natural Sciences, University of Buenos Aires (FCEN-UBA), Buenos Aires, Argentina*
[2]*National Council of Scientific and Technical Research (CONICET), Buenos Aires, Argentina*

Correspondence should be addressed to Patricio Santagapita; prs@di.fcen.uba.ar

Received 29 June 2016; Accepted 14 August 2016

Academic Editor: Yi-Hung Chen

Copyright © 2016 T. Aguirre Calvo and P. Santagapita. This is an open access article distributed under the Creative Commons Attribution License, which permits unrestricted use, distribution, and reproduction in any medium, provided the original work is properly cited.

Alginate hydrogels are suitable for the encapsulation of a great variety of biomolecules. Several alternatives to the conventional alginate formulation are being studied for a broad range of biotechnological applications; among them the addition of sugars and biopolymers arises as a good and economic strategy. Sugars (trehalose and β-cyclodextrin), a cationic biopolymer (chitosan), an anionic biopolymer (pectin), and neutral gums (Arabic, guar, *espina corona*, and *vinal* gums) provided different characteristics to the beads. Here we discuss the influence of beads composition on several physicochemical properties, such as size and shape, analyzed through digital image analysis besides both water content and activity. The results showed that the addition of a second biopolymer, β-CD, or trehalose provoked more compact beads, but the fact that they were compact not necessarily implies a concomitant increase in their circularity. *Espina corona* beads showed the highest circularity value, being useful for applications which require a controlled and high circularity, assuring quality control. Beads with trehalose showed lower water content than the rest of the system, followed by those containing galactomannans (*espina corona*, *vinal*, and guar gums), revealing polymer structure effects. A complete characterization of the beads was performed by FT-IR, assigning the characteristics bands to each individual component.

1. Introduction

Considerable research has been conducted in the field of encapsulation leading to studies on the protection and controlled release of bioactive compounds used in pharmaceutical, cosmetic, and food industry [1, 2]. There has been great interest in the use of hydrogel beads that contained encapsulated agents, being the search of adequate excipients that assure stability and controlled release a great challenge. Several hydrocolloids and biopolymers are used for this purpose due to their properties related to wall protection and delivery as well as their functional and sensory attributes. Among them, sodium alginate (isolated from brown algae) is one of the most used excipients for formulating hydrogel beads due to its encapsulating/gelling properties when cross-linked with divalent ions like calcium [3], leading to a huge range of possibilities, since it possesses several advantages compared with other commonly used biopolymers listed below: (a) easy and low-cost preparation method, which consists of dropping an aqueous solution (or emulsion) of the biopolymer and bioactive compound into $CaCl_2$ [4, 5]; (b) compatibility with other excipients, increasing its wall and release properties; (c) versatility, by allowing encapsulation of a wide range of bioactive compound, which are highly sensitive to environmental conditions, since the interior is known to be chemically inert [6]; (d) nontoxicity and biodegradability, since results of *in vivo* studies demonstrated the development of a biodegradable alginate carrier system for antibiotics and bone cells, providing a potential treatment procedure for infected bone defects [7]. However, some disadvantages are often associated with this carrier, including high biomolecule leakage, low mechanical strength, and large pore size [8].

In order to optimize the encapsulation efficiency and control release of biocompounds, the addition of sugars and biopolymers arises as a good and economic strategy. Among sugars, trehalose, a disaccharide used as cryo- and

dehydroprotective agent, has been proven to improve the formulation and protect enzymes during freezing and thermal treatment on alginate beads [5, 9], and β-cyclodextrin, cyclic oligosaccharides composed of seven glucopyranose units, possesses the ability to encapsulate hydrophobic molecules with suitable size inside their cavity to form inclusion complexes [10]. Among the biopolymers, chitosan is one of the most used, since a cationic biopolymer provides thicker membranes for the direct interaction with alginate, modifying also some thermal [5] and functional properties [11]. An anionic biopolymer such as pectin, similarly to alginate, forms hydrogel following the egg-box model [12], competing for Ca(II) with alginate to form the gelation network, affecting functional properties [5]. It is known that the inclusion of food gums on mixtures of emulsions to form beads has advantages showing a more rigid structure and at the same time protects the compound from diffusion [13]; then, the inclusion of four neutral gums was assessed: guar and Arabic gums, which are two of the most used gums, and two novel gums, *vinal* and *espina corona gums*. The latter gums are novel nongelling biopolymers that provide high viscosity to aqueous solutions and are relatively stable against variations in pH, ionic strength, and temperature [14–16].

The purpose of the present work was to assess the influence of beads composition on several physicochemical properties, such as size and shape, analyzed through digital image analysis, as well as both water content and activity. A complete characterization of the beads was performed by FT-IR, assigning the characteristics bands to each one of the individual components.

2. Materials and Methods

2.1. Materials. The employed materials are listed below: *sodium alginate* (Algogel 5540) Cargill SA (San Isidro, Buenos Aires, Argentina), MW = 1,97.10^5 g/mol and mannuronate/guluronate ratio = 0.6; *D-trehalose dihydrate* (Hayashibara Co., Ltd., Shimoishii, Okayama, Japan/Cargill Inc., Minneapolis, Minnesota, USA), MW = 378 g/mol; *β-cyclodextrin* (*β-CD*) (Amaizo American Maize-Products Co., Hammond, IN, USA), MW = 1185 g/mol; *low methoxyl pectin* (*LM*), Meath & Nutrition Degussa Argentina Inc. (San Isidro, Buenos Aires, Argentina) with esterification degree between 26 and 31% and amidation degree between 16 and 19%; guar gum (Cordis SA, Villa Luzuriaga, Buenos Aires, Argentina), MW ~ 220,000 g/mol and M/G (mannose/galactose) = 1.8; Arabic gum (Biopack, Zárate, Buenos Aires, Argentina). MW ~ 250,000 g/mol and purity of 99%; *espina corona gum* was provided from Supply Idea Argentina S.A. (Chaco, Argentina), with the following percentage composition: moisture, 0.04 g/100 g; ashes, 1.44 g/100 g; fat, 0.27 g/100 g; protein, 2.17 g/100 g; crude fiber, 0.70 g/100 g; polysaccharides, 85.38 g/100 g; and M/G = 2.5 [16]; *chitosan,* medium molecular weight viscosity of 200–800 cP (1% w/v in 1% acetic acid at 25°C, Brookfield viscometer), and degree of deacetylation of 75–85% (Sigma-Aldrich Chemie GmbH, Steinheim, Germany). *Vinal gum* is a gum extracted from seeds of *Prosopis ruscifolia* as reported by Busch et al. [14], with M/G = 1.6, protein content of 1.9 ± 0.2% (w/w), and MW of $1.43 \cdot 10^6$ Da.

Extra virgin olive oil (Molino Cañuelas SACIFIA, Mendoza, Argentina) was purchased in the local market to formulate emulsions. The emulsions were prepared in an Ultra-Turrax T18B (IKA-Werke GMBH & CO.KG, Staufen, Germany) at 15,500 rpm (speed 4) for a period of 10 min. The oil was emulsified with the corresponding biopolymer solution in a mass ratio of 1 : 2.

2.2. Preparation of Alginate Beads. The formulations of initial emulsions were 1% (w/v) alginate with 20% (w/v) trehalose mixed with 0.25% (w/v) of pectin, guar, Arabic, *vinal*, or *espina corona* gums.

Alginate solutions were mixed with the biopolymers to generate initial emulsions. For all the formulation a 1% (w/v) solution of sodium alginate was prepared with bidistilled water in a magnetic stirrer allowing full hydration of the alginate for about 12 h; to remove any air bubbles the solution was sonicated for 3 min. Beads were prepared by ionotropic gelation according to the drop method described previously [5, 9]. Briefly, to ensure bead generation a 2.5% (w/v) $CaCl_2$ solution (with trehalose 20% (w/v), in addition to 1.5% (w/v) β-cyclodextrin or 0.5% (w/v) chitosan for the correspondent systems) was prepared in bidistilled water as an external medium. By dripping 10 mL of the solution of the initial emulsion was performed using a peristaltic pump with model BT50-1J JY10 head (Boading Longer Precision Pump Co., Ltd., China), always with constant stirring, a standard pipette tip for 0.1–10 μL (0.35 mm diameter) connected to a silicone tube 1 mm internal diameter (3 mm external) over 100 mL of $CaCl_2$ solution.

The systems were generated at pH higher than 4, considering the pk_a values of alginate (3.38 and 3.65 [5, 9]). pH values were between 5.5 and 6 for A and A-T beads and between 4 and 5 for the rest of the beads.

2.3. Size and Shape through Digital Image Analysis. The size and shape of the beads were obtained by analyzing the digital images captured by a digital camera (Canon digital camera, 3.2 Mpix PowerShotA70; Canon Inc., Malaysia; with zoom fixed at 3x) coupled to a binocular microscope (Unitron MS, Unitron Inc., New York, USA; magnification at 7x). The pictures were analyzed with the free license software ImageJ. Once beads images are capture for all formulations, the size and shape were obtained with the image analysis, processing with free license software ImageJ (http://rsbweb.nih.gov/ij/). The performed analysis is shown in Figure 1.

Area, perimeter, Feret's diameter, and circularity were analyzed for at least 60 beads by applying the "analyze particle" command of the software. Feret's diameter corresponds to the longest distance between any two points along the bead boundary. Circularity is defined as a value between 0 and 1 indicating how closely the shape of the particle resembles a circle. The effect of composition on Feret's diameter and circularity were analyzed by 1-way ANOVA with Tukey post test using Prism 5 (GraphPad Software Inc.). The significant differences between values with $p < 0.05$ were indicated on

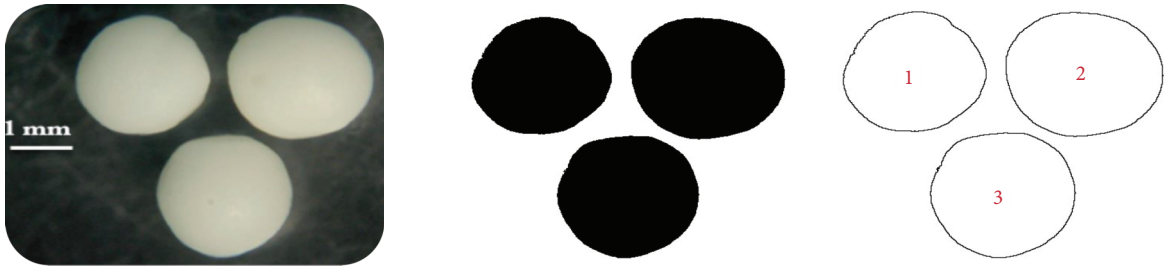

Figure 1: Sequence of image analysis from the original image to the particle analysis. For example, beads containing only alginate (A) as biopolymer.

columns by different letters, "a" being the higher value. The statistical analysis was adapted from [5, 9, 14]. The ImageJ software was calibrated to transform the measured pixels in length units (mm) by taking pictures of a caliper section.

2.4. Water Content and Water Activity. The total water content of the beads was determined gravimetrically by difference in weight before and after drying in vacuum oven for 48 h at 96 ± 2°C. The water content was expressed in percentage of grams of water per gram of sample (wet basis, w.b.).

Water activity (a_w) was determined by means of an Aqualab instrument (Decagon Devices, Inc., USA).

Water content and a_w were measured in triplicate. The effect of composition on water content and a_w was analyzed by 1-way ANOVA with Tukey post test using Prism 5 (GraphPad Software Inc.). The significant differences between values with $p < 0.05$ were indicated in columns by different letters.

2.5. Attenuated Total Reflectance-Fourier Transform-Infrared Spectroscopy (FT-IR). FT-IR spectra were measured on a Spectrum 400 spectrometer FT-IR/FT-NIR (Perkin Elmer, Inc., Shelton, CT, USA). Wet beads were subjected to freeze-drying prior to analysis due to the high absorption of water which strongly dominates the spectrum, masking biopolymers and sugars bands. Sugars and biopolymers solutions were also freeze-dried to obtain control spectra for each excipient. All the samples were studied in a MIRacle attenuated total reflectance (ATR) accessory (PIKE Technologies, Inc., Madison, WI, USA) with a diamond/ZnSe crystal of single reflection at an incident angle of 45°. Two beads were placed directly thereon, without prior sample preparation, obtaining a very good signal to noise ratio. The spectra were acquired in reflection mode between 675 and 4000 cm^{-1}, acquiring 32 scans averaged with a resolution of 4 cm^{-1}. A strong apodization was used, with a magnitude phase correction. A flat tip was employed to obtain an intimate contact between sample and crystal, without pressure control. A background spectrum was recorded in air (without sample) prior to each spectrum measurement. Spectral analysis was performed using the Spectrum software version 6.3.5 (PerkinElmer, Inc.). The average of triplicates for each system was reported. Baseline was corrected and the spectra were normalized (between 0 and 1) for figure presentation.

3. Results and Discussion

3.1. Size and Shape through Digital Image Analysis. Alginate macrobeads of different formulations obtained by the drop method were analyzed by image analysis. The size and morphological characterization of the beads are relevant since they could have impact on different physicochemical properties such as water sorption and release of the encapsulated agent as well as consumer's acceptance (improve the aesthetic quality which could be a desirable characteristic for pharmaceutical, food, and feed products) [17]. Figure 2 shows size (determined as Feret's diameter), circularity, area, and perimeter of the beads analyzed by optical microscopy and a digital image processing technique.

The addition of any excipient to alginate resulted in significant reduction of the diameter and the area and perimeter of the beads, as shown in Figure 2. Alginate beads showed a significant deviation from sphericity (circularity values of 0.6), showing characteristics of an ellipse. The addition of any excipient to alginate caused an increase in the circularity (Figure 2(b)), except for trehalose in A-T beads, since there are no significant differences between them (A versus A-T). This increment of bead circularity due to the addition of a second biopolymer or β-CD was probably related to changes in the surface tension/viscosity of the droplets containing the initial emulsion, which was further used to form alginate beads.

It is interesting to note that the addition of a second biopolymer, β-CD, or trehalose provoked more compact beads, but the fact that they were compact not necessarily implies a concomitant increase in their circularity. For example, AVG-T beads showed a smaller diameter compared to A-T ones (being both diameters smaller than A beads), showing no significant differences in circularity from each other. Beads containing Arabic gum or β-CD were shown to be the smaller ones for all the analyzed parameters (area, perimeter,

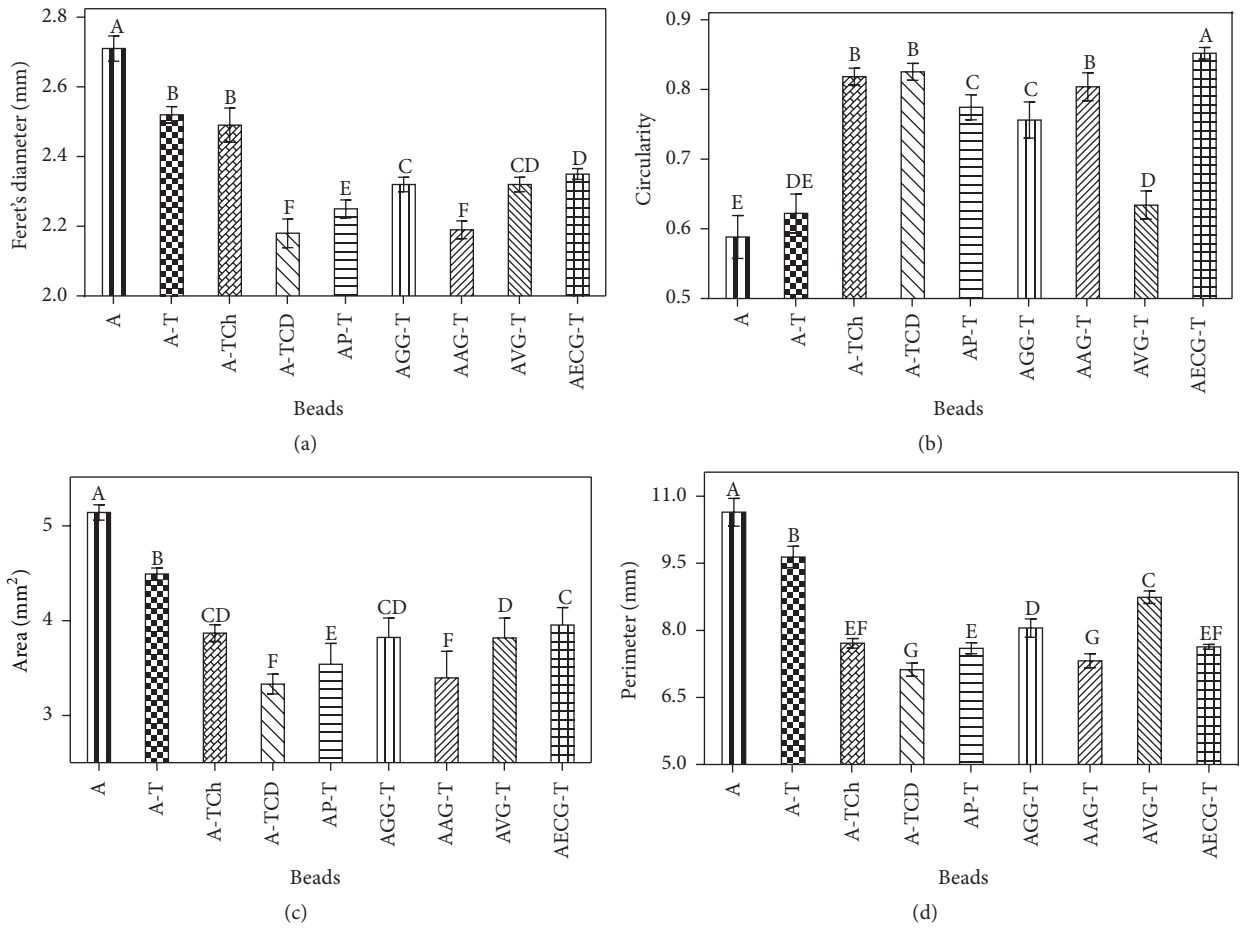

Figure 2: Feret's diameter (a), circularity (b), area (c), and perimeter (d) obtained by image analysis of the beads of different composition. Confidence intervals at 95% are indicated. At least, 60 beads of each system were analyzed. Different letters on the columns (A–G, being highest to lowest values, resp.) indicate significant differences between values with $p < 0.05$.

or diameter). Beads containing *espina corona* gum showed the highest value of circularity (0.85).

3.2. Water Activity and Content. It is critical to know the water content and water activity (a_w) of beads to define the appropriate processing and storage conditions, considering the high influence of water on stability when formulations containing bioactive compounds are stored [9]. a_w and the water content were analyzed according to the composition of the beads, as shown in Table 1. As expected, the wet beads showed high a_w values between 0.96 and 0.98 but lower than the values reported by other authors for alginate beads (around 0.99) [9, 18], probably due to the presence of oil in the beads. Most of the beads containing sugars and biopolymers had lower a_w values than A beads (except for A-TCh and AP-T beads) showing that the addition of other soluble components caused a decrease in a_w. However, not all the beads had lower water content values than A beads. This difference is possible due to the fact that the beads of different systems probably had differences in their water sorption isotherms, which were not determined in this study. The beads with trehalose (A-T) showed lower water content than the rest of the system, followed by those containing galactomannans (*espina corona*, *vinal*, and guar gums).

3.3. Component Identification by FT-IR. The individual components of the extract and of the beads were determined by FT-IR using a micro-ATR (attenuated total reflectance) accessory. The advantage of this device is that it allows the direct measurement of the beads, without the need to use dispersants matrices (such as the commonly used KBr), simplifying sample preparation and subsequent processing of data.

Figures 3 and 4 show the spectra of the freeze-dried beads and the correspondent freeze-dried controls of each employed excipient. The signals corresponding to the presence of oil are clearly seen in all beads spectra (Figures 3 and 4), confirming the correct incorporation of the emulsions in the beads. In these spectra, characteristic bands associated with lipid groups were observed between 1380 and 1370, 1485 and 1430 cm^{-1} (CH bending), 1745 cm^{-1} (C=O, ester) and 3010, and 2920 and 2852 cm^{-1} (CH stretch) and a major band at 1160 cm^{-1}. Besides, it is possible to observe the presence of each of the different excipients used in each bead system from the recognition of the corresponding major signals as well

Table 1: Water content (as percent of wet basis, WC % w.b.) and water activity (a_w) obtained for different beads formulations. Standard deviation values ($n = 3$) are included.

Beads	WC (% w.b.)	a_w
A	$44 \pm 2^{(a)}$	$0.983 \pm 0.002^{(a)}$
A-T	$37 \pm 1^{(d)}$	$0.975 \pm 0.002^{(b)}$
A-TCh	$41 \pm 2^{(a,b)}$	$0.981 \pm 0.004^{(a,b)}$
A-TCD	$41 \pm 1^{(a,b)}$	$0.979 \pm 0.002^{(a,b)}$
AP-T	$39 \pm 3^{(a,b,c,d)}$	$0.981 \pm 0.002^{(a)}$
AGG-T	$39 \pm 1^{(b,c,d)}$	$0.967 \pm 0.003^{(c)}$
AAG-T	$41.6 \pm 0.6^{(a)}$	$0.958 \pm 0.006^{(c,d)}$
AVG-T	$40 \pm 2^{(a,b,c,d)}$	$0.960 \pm 0.003^{(d)}$
AECG-T	$37.1 \pm 0.6^{(c,d)}$	$0.961 \pm 0.007^{(c,d)}$

Different letters (a–d) indicate significant differences between values in each column with $p < 0.05$, assigning (a) to the highest and (d) to the lowest values.

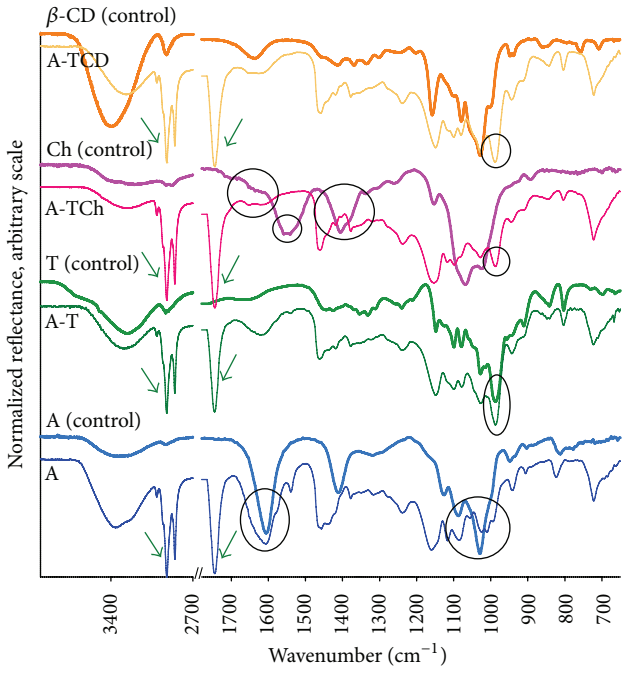

Figure 3: Normalized spectra obtained from freeze-dried beads and their control (freeze-dried biopolymers or sugars). Characteristics bands are highlighted by circles and arrows (lipids).

as the already reported interaction between chitosan and alginate [5, 18] through peak shifts in A-TCh beads (Figure 3).

The characteristic bands of alginate correspond to its carboxylic groups at 1595 and 1405 cm^{-1} (symmetric and asymmetric stretching, resp.) [19, 20] and have been observed also in A beads spectra. These signals are less intense in the rest of the beads spectra (Figures 3 and 4) due to the presence of trehalose, whose signals strongly dominate the spectra (bands at 983 cm^{-1} and 1148 cm^{-1}, corresponding to the glycosidic bond, [21]). The band at 1033 cm^{-1} corresponding to CO stretching is characteristic of alginate as well [20, 21]. The signals at 1490–1380 cm^{-1} correspond to both alginate and oil.

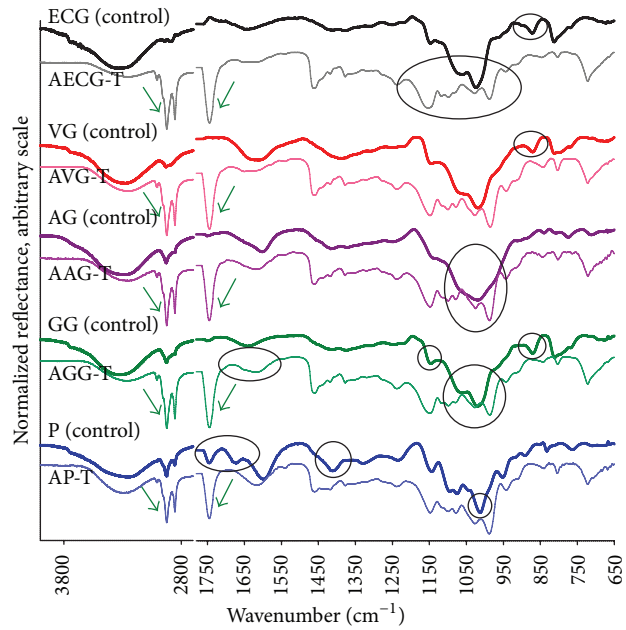

Figure 4: Normalized spectra obtained from freeze-dried beads and their control (freeze-dried biopolymers or sugars). Characteristics bands are highlighted by circles and arrows (lipids).

A signal shift was observed for the signal at 1033 cm^{-1}, which generated a characteristic three peaks pattern at 1024, 1007, and 992 cm^{-1}.

It is important to consider that the employed biopolymers present some similarities (hydrocolloid behavior, major composition of sugars, and low protein content (except for Arabic gum)). These similarities lead to similar bands in the IR-spectra, but some characteristic signals (detailed below) still can be observed. Besides, the 1500–900 cm^{-1} region was not disturbed by the presence of water and it is very rich in terms of structural information, as many characteristic functional groups of saccharides signals appeared in this spectral region [21].

Chitosan spectrum shows an absorption peak marked at 1550 cm^{-1} due to the protonation of the amino group, one at 1635 cm^{-1} due to the amide bond, and the deformation of the CH_2 groups occurring at 1405 cm^{-1} [20, 22]. The evidence of the interaction between alginate and chitosan can be seen in the A-TCh beads in the displacement and broadening of these bands (1641–1610 cm^{-1} and 1405–1420 cm^{-1}), although the last one is superposed due to contribution of oil band.

Signals characteristics of pectin are 1741 (C=O vibration of the COOH), 1605 (symmetric vibration of COO-), 1410 (antisymmetric vibration of COO-), and 1011 cm^{-1} (stretching C=O) [23, 24]. Unlike what was observed with the chitosan, for pectin beads (AP-T), there was no displacement of bands because both were negatively charged and do not form a complex (as expected). However, the AP-T beads show more intense bands at 1415 and 1330 cm^{-1} (which are quite small in the scale presented) than the AT beads possibly due to the contribution of pectin.

The spectra of gums, especially for the three galactomannans (guar, *espina corona*, and *vinal* gums), showed similarities in the carbohydrate region (1200–700 cm^{-1}), especially in the signals corresponding to the anomeric carbons of the different monomers (specific signals for galactose (α o β) at 871 ± 7 cm^{-1}, mannose (876 ± 9 cm^{-1}), and glucose (915, 874, and 767 ± 8 cm^{-1})) [25–27]. The relative intensity of bands at 1150, 1070, and 970 cm^{-1} with respect to the major band at 1020 cm^{-1} was related to the differences in the mannose/galactose ratios of the employed galactomannans. The main bands of guar gum were observed at 1017, 1082, and 1158 cm^{-1} (C-OH stretching), at 1648 cm^{-1} (observed as a shoulder in AGG-T), and at 1620 cm^{-1} (OH bending). Furthermore, AGG-T beads showed a broadening of the band at 1150 cm^{-1}. Arabic gum spectrum showed characteristic bands at 3000–3600 cm^{-1} (O-H stretching), 2993 and 2918 cm^{-1} (C-H stretching), and 1612 cm^{-1} (C=O stretching) with a main peak at 1017 cm^{-1}.

To the best of our knowledge, FT-IR spectra of *vinal* and *espina corona* gums are reported for the very first time. *Vinal* gum spectrum showed a very broad signal between 1700 and 1500 cm^{-1}, which includes several peaks with maxima between 1600 and 1630 cm^{-1}. In the AVG-T beads, the shape of the broad band at 1620 cm^{-1} was more alike to that of *vinal* gum than that of alginate, showing a relative increase at 1640 cm^{-1} (in comparison to the band at 1620 cm^{-1}). A widening of the signal at 1150 cm^{-1} (coincident with the presence of a band in the *espina corona* control spectrum) and a relative modification of the ratio of the three bands pattern (region 1060–1130 cm^{-1}) were observed for the beads containing *espina corona* gum (Figure 4).

4. Conclusions

Shape and size of the beads were strongly affected by the composition. The addition of a second biopolymer, β-cyclodextrin, or trehalose causes more compact beads, but this does not necessarily imply an increase in circularity. Beads with Arabic gum or β-CD were shown to be the smaller ones. Beads containing *espina corona* showed the highest value of circularity, which could be useful for applications which require a controlled and high circularity, assuring quality control.

The addition of sugars and neutral biopolymers produced lower a_w values than plain alginate beads. However, there were no concomitant lower water content values. This difference is possible due to the fact that the beads of different systems probably had differences in their water sorption isotherms. Then, it is important to keep in mind that the addition of excipients could also have impact on other physicochemical characteristics that, in turn, could affect the physicochemical properties most commonly analyzed.

The obtained results represent the starting point to overcome the disadvantages associated with alginate as a carrier, leading to a higher stability and controlled release of the alginate-Ca(II) beads by using a second biopolymer, β-cyclodextrin, or trehalose.

Components of the beads were successfully determined by infrared spectroscopy studies of Fourier transform (FT-IR). This study allows us to observe the interaction between chitosan and alginate and the presence of each of the components used in the preparation of the beads from the identification of its main bands.

Abbreviation List

A: Alginate
T: Trehalose
Ch: Chitosan
CD: β-Cyclodextrin
P: Pectin
GG: Guar gum
AG: Arabic gum
VG: *Vinal* gum
ECG: *Espina corona* gum.

Competing Interests

The authors declare that there is no conflict of interests regarding the publication of this paper.

Acknowledgments

The authors acknowledge the financial support of ANPCYT (PICT 2013 no. 0434 and PICT 2013-1331) and CONICET and UBA (Project UBACyT 20020130100443BA). They also acknowledge Dr. Pilar Buera for the useful discussions and Dr. Verónica Busch for *vinal* gum donation.

References

[1] B. Zeeb, A. H. Saberi, J. Weiss, and D. J. McClements, "Retention and release of oil-in-water emulsions from filled hydrogel beads composed of calcium alginate: impact of emulsifier type and pH," *Soft Matter*, vol. 11, no. 11, pp. 2228–2236, 2015.

[2] B. Zeeb, A. H. Saberi, J. Weiss, and D. J. McClements, "Formation and characterization of filled hydrogel beads based on calcium alginate: factors influencing nanoemulsion retention and release," *Food Hydrocolloids*, vol. 50, pp. 27–36, 2015.

[3] M. H. L. Ribeiro, C. Afonso, H. J. Vila-Real, A. J. Alfaia, and L. Ferreira, "Contribution of response surface methodology to the modeling of naringin hydrolysis by naringinase Ca-alginate beads under high pressure," *LWT—Food Science and Technology*, vol. 43, no. 3, pp. 482–487, 2010.

[4] E.-S. Chan, B.-B. Lee, P. Ravindra, and D. Poncelet, "Prediction models for shape and size of Ca-alginate macrobeads produced through extrusion-dripping method," *Journal of Colloid and Interface Science*, vol. 338, no. 1, pp. 63–72, 2009.

[5] P. R. Santagapita, M. F. Mazzobre, and M. D. P. Buera, "Invertase stability in alginate beads: effect of trehalose and chitosan inclusion and of drying methods," *Food Research International*, vol. 47, no. 2, pp. 321–330, 2012.

[6] L. G. Griffith, "Polymeric biomaterials," *Acta Materialia*, vol. 48, no. 1, pp. 263–277, 2000.

[7] S. W. N. Ueng, M. S. Lee, S.-S. Lin, E.-C. Chan, and S.-J. Liu, "Development of a biodegradable alginate carrier system for antibiotics and bone cells," *Journal of Orthopaedic Research*, vol. 25, no. 1, pp. 62–72, 2007.

[8] M. M. M. Elnashar, E. N. Danial, and G. E. A. Awad, "Novel carrier of grafted alginate for covalent immobilization of inulinase," *Industrial and Engineering Chemistry Research*, vol. 48, no. 22, pp. 9781–9785, 2009.

[9] P. R. Santagapita, M. F. Mazzobre, and M. P. Buera, "Formulation and drying of alginate beads for controlled release and stabilization of invertase," *Biomacromolecules*, vol. 12, no. 9, pp. 3147–3155, 2011.

[10] P. A. Ponce Cevallos, M. P. Buera, and B. E. Elizalde, "Encapsulation of cinnamon and thyme essential oils components (cinnamaldehyde and thymol) in β-cyclodextrin: effect of interactions with water on complex stability," *Journal of Food Engineering*, vol. 99, no. 1, pp. 70–75, 2010.

[11] P. R. Santagapita, M. F. Mazzobre, and M. P. Buera, "Stabilization and controlled release of invertase through the addition of trehalose in wet and dried alginate-chitosan beads," in *Water Stress in Biological, Chemical, Pharmaceutical and Food Systems: ISOPOW '11*, G. Gutiérrez, G. Barbosa-Cánovas, L. Alamilla, E. Para-Arias, and M. P. Buera, Eds., pp. 353–360, Springer, 2015.

[12] I. Braccini, R. P. Grasso, and S. Pérez, "Conformational and configurational features of acidic polysaccharides and their interactions with calcium ions: a molecular modeling investigation," *Carbohydrate Research*, vol. 317, no. 1–4, pp. 119–130, 1999.

[13] I. Roy, M. Sardar, and M. N. Gupta, "Cross-linked alginate-guar gum beads as fluidized bed affinity media for purification of jacalin," *Biochemical Engineering Journal*, vol. 23, no. 3, pp. 193–198, 2005.

[14] V. M. Busch, A. A. Kolender, P. R. Santagapita, and M. P. Buera, "*Vinal* gum, a galactomannan from *Prosopis ruscifolia* seeds: physicochemical characterization," *Food Hydrocolloids*, vol. 51, pp. 495–502, 2015.

[15] V. M. Busch, F. Loosli, P. R. Santagapita, M. P. Buera, and S. Stoll, "Formation of complexes between hematite nanoparticles and a non-conventional galactomannan gum. Toward a better understanding on interaction processes," *Science of the Total Environment*, vol. 532, pp. 556–563, 2015.

[16] M. J. Perduca, M. J. Spotti, L. G. Santiago, M. A. Judis, A. C. Rubiolo, and C. R. Carrara, "Rheological characterization of the hydrocolloid from *Gleditsia amorphoides* seeds," *LWT—Food Science and Technology*, vol. 51, no. 1, pp. 143–147, 2013.

[17] B.-B. Lee, P. Ravindra, and E.-S. Chan, "Size and shape of calcium alginate beads produced by extrusion dripping," *Chemical Engineering and Technology*, vol. 36, no. 10, pp. 1627–1642, 2013.

[18] L. Deladino, P. S. Anbinder, A. S. Navarro, and M. N. Martino, "Encapsulation of natural antioxidants extracted from *Ilex paraguariensis*," *Carbohydrate Polymers*, vol. 71, no. 1, pp. 126–134, 2008.

[19] M. G. Sankalia, R. C. Mashru, J. M. Sankalia, and V. B. Sutariya, "Papain entrapment in alginate beads for stability improvement and site-specific delivery: physicochemical characterization and factorial optimization using neural network modeling," *AAPS PharmSciTech*, vol. 6, no. 2, pp. E209–E222, 2005.

[20] B. Sarmento, D. Ferreira, F. Veiga, and A. Ribeiro, "Characterization of insulin-loaded alginate nanoparticles produced by ionotropic pre-gelation through DSC and FTIR studies," *Carbohydrate Polymers*, vol. 66, no. 1, pp. 1–7, 2006.

[21] M. Kačuráková and M. Mathlouthi, "FTIR and laser-Raman spectra of oligosaccharides in water: characterization of the glycosidic bond," *Carbohydrate Research*, vol. 284, no. 2, pp. 145–157, 1996.

[22] B. Smitha, S. Sridhar, and A. A. Khan, "Chitosan-sodium alginate polyion complexes as fuel cell membranes," *European Polymer Journal*, vol. 41, no. 8, pp. 1859–1866, 2005.

[23] A. Sinitsya, J. Čopíková, V. Prutyanov, S. Skoblya, and V. MacHovič, "Amidation of highly methoxylated citrus pectin with primary amines," *Carbohydrate Polymers*, vol. 42, no. 4, pp. 359–368, 2000.

[24] T. H. Kim, Y. H. Park, K. J. Kim, and C. S. Cho, "Release of albumin from chitosan-coated pectin beads in vitro," *International Journal of Pharmaceutics*, vol. 250, no. 2, pp. 371–383, 2003.

[25] S. Paul and G. S. Mittal, "Regulating the use of degraded oil/fat in deep-fat/oil food frying," *Critical Reviews in Food Science and Nutrition*, vol. 37, no. 7, pp. 635–662, 1997.

[26] H. T. Pedersen, L. Munck, and S. B. Engelsen, "Low-field ^{1}H nuclear magnetic resonance and chemometrics combined for simultaneous determination of water, oil, and protein contents in oilseeds," *Journal of the American Oil Chemists' Society*, vol. 77, no. 10, pp. 1069–1076, 2000.

[27] W. S. Price, "Pulsed-field gradient nuclear magnetic resonance as a tool for studying translational diffusion: part 1. Basic theory," *Concepts in Magnetic Resonance*, vol. 9, no. 5, pp. 299–335, 1997.

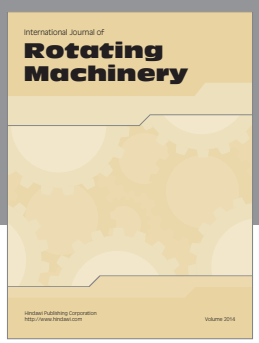

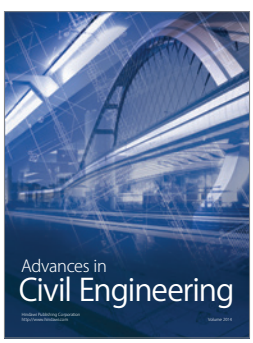

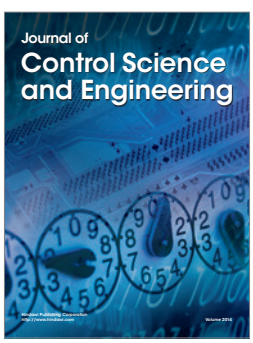

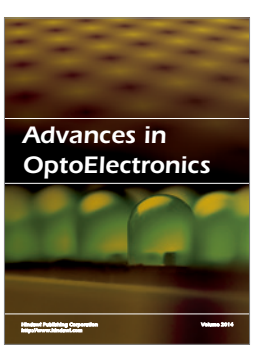

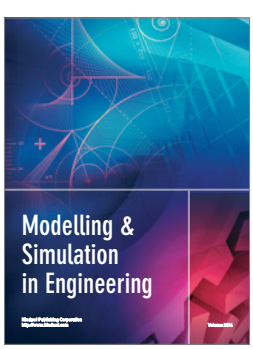

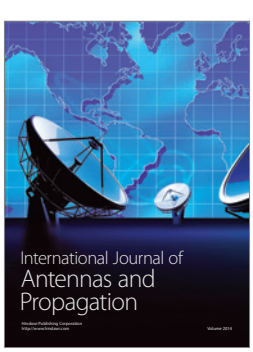

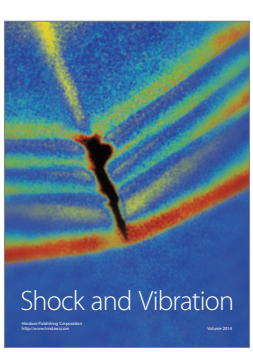

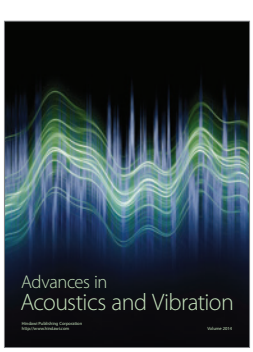

Hindawi

Submit your manuscripts at
http://www.hindawi.com